Spectral density of polychromatic electromagnetic waves

L. E. Helseth
Division of Physics and Applied Physics, School of Physical and Mathematical Sciences, Nanyang Technological University, Singapore
(Received 3 November 2005; published 3 February 2006)

We investigate theoretically how the vectorial nature of polychromatic electromagnetic fields results in polarization components with different spectral characteristics, thus leading to redshifts, blueshifts, and spectral distributions with multiple peaks. We discuss how these effects can be used to design spatially localized spectra with tailored spectral densities.

DOI: 10.1103/PhysRevE.73.026602 PACS number(s): 41.20.Jb

I. INTRODUCTION

With an increasing number of new applications, it becomes more and more important to understand the properties of polychromatic light. Both pulsed and continuous waves play fundamental roles in a number of spectroscopic systems, and it is therefore necessary to probe their spectral distributions [1–13]. Recent studies have demonstrated that spectral changes can take place in various classes of polychromatic scalar waves propagating in free space [1–3]. In particular, it was shown that diffracted waves exhibit drastic spectral shifts near regions of zero intensity, thus resulting in a number of interesting spectral characteristics [1–6]. Here we aim at studying the influence of the electromagnetic character on such spectral shifts. In particular we show that interfering waves with different wave vectors will in general exhibit electric field components with different spectral densities. This fact can be used to shape the light in, e.g., a Michelson interferometer, where the path difference between the waves play an essential role. We also show that the polarization distribution of a strongly focused wave will fundamentally alter the spectral density of the waves. These phenomena may help us shaping the spectral density of a wave, both globally and locally, and could therefore be of interest in spectroscopic systems.

II. SPECTRAL DENSITY OF INTERFERING PLANE WAVES

Consider two waves with propagation vectors $\boldsymbol{k}_1 = -k \sin\theta\,\hat{\boldsymbol{e}}_x + k\cos\theta\,\hat{\boldsymbol{e}}_z$ and $\boldsymbol{k}_2 = k\sin\theta\,\hat{\boldsymbol{e}}_x + k\cos\theta\,\hat{\boldsymbol{e}}_z$, where k is the wave number and θ is the half-angle between the propagation vectors. The geometry is shown in Fig. 1, which also shows the directions of the electric field vectors. The two waves have the same amplitude, but travel different paths (as in a Michelson interferometer), thus resulting in a time lag $\tau = s/c$ between them, where s is the path difference and c is the speed of light. The two interfering waves have electric field vectors $\boldsymbol{E}_1(\boldsymbol{r},t)$ and $\boldsymbol{E}_2(\boldsymbol{r},t-\tau)$. The total field $\boldsymbol{E}(\boldsymbol{r},t) = E_x(\boldsymbol{r},t)\hat{\boldsymbol{e}}_x + E_z(\boldsymbol{r},t)\hat{\boldsymbol{e}}_z$ is a sum of the two interfering fields $\boldsymbol{E}(\boldsymbol{r},t) = \boldsymbol{E}_1(\boldsymbol{r},t) + \boldsymbol{E}_2(\boldsymbol{r},t-\tau)$. We write the electric field vectors as

$$\boldsymbol{E}_1(\boldsymbol{r},t) = E_1(\boldsymbol{r},t)\cos\theta\,\hat{\boldsymbol{e}}_x + E_1(\boldsymbol{r},t)\sin\theta\,\hat{\boldsymbol{e}}_z \tag{1}$$

and

$$\boldsymbol{E}_2(\boldsymbol{r},t-\tau) = E_2(\boldsymbol{r},t-\tau)\cos\theta\,\hat{\boldsymbol{e}}_x - E_2(\boldsymbol{r},t-\tau)\sin\theta\,\hat{\boldsymbol{e}}_z, \tag{2}$$

where $\hat{\boldsymbol{e}}_x$ and $\hat{\boldsymbol{e}}_z$ are unit vectors in the x and z directions, respectively. In the complex analytic representation the electric field vector can be written as

$$\boldsymbol{E}(\boldsymbol{r},t) = \int_0^\infty \tilde{\boldsymbol{E}}(\boldsymbol{r},\omega)\exp(i\boldsymbol{k}\cdot\boldsymbol{r} - i\omega t)d\omega, \tag{3}$$

where

$$\tilde{\boldsymbol{E}}(\omega) = \frac{1}{2\pi}\int_0^\infty \boldsymbol{E}(t)\exp(i\omega t)d\omega. \tag{4}$$

We can now write the x and z components of the total field as

$$E_x(\boldsymbol{r},t) = \cos\theta\int_0^\infty \tilde{E}_0(\boldsymbol{r},\omega)[\exp(i\boldsymbol{k}_1\cdot\boldsymbol{r}) + \exp(i\boldsymbol{k}_2\cdot\boldsymbol{r} + i\omega\tau)]\exp(-i\omega t)d\omega \tag{5}$$

and

$$E_z(\boldsymbol{r},t) = \sin\theta\int_0^\infty \tilde{E}_0(\boldsymbol{r},\omega)[\exp(i\boldsymbol{k}_1\cdot\boldsymbol{r}) - \exp(i\boldsymbol{k}_2\cdot\boldsymbol{r} + i\omega\tau)]\exp(-i\omega t)d\omega, \tag{6}$$

where $\tilde{E}_0(\boldsymbol{r},\omega) = \tilde{E}_1(\boldsymbol{r},\omega) = \tilde{E}_2(\boldsymbol{r},\omega)$ since the two interfering beams have the same amplitude. The time-independent, average intensity of the electromagnetic wave is proportional to $\langle|\boldsymbol{E}(t)|^2\rangle$, and we will therefore write $I = \langle|\boldsymbol{E}(\boldsymbol{r},t)|^2\rangle$, where $\langle\cdots\rangle$ denotes the average. We will also require that the field is stationary, so that $\langle\tilde{E}_0(\boldsymbol{r},\omega_1)\tilde{E}_0^*(\boldsymbol{r},\omega_2)\rangle = S^i(\boldsymbol{r},\omega_1)\delta(\omega_1-\omega_2)$,

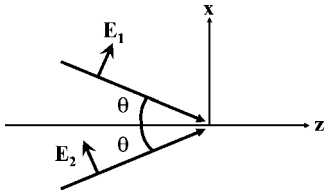

FIG. 1. Two waves with different propagation directions and electric field vectors are interfering.

where $S^i(\boldsymbol{r},\omega_1)$ is the incident spectral density of the two beams. It can now be seen that

$$\langle|E_x|^2\rangle = 2\cos^2\theta\int_0^\infty S^i(\boldsymbol{r},\omega)\left[1+\cos\left(2kx\sin\theta+\omega\frac{s}{c}\right)\right]d\omega \tag{7}$$

and

$$\langle|E_z|^2\rangle = 2\sin^2\theta\int_0^\infty S^i(\boldsymbol{r},\omega)\left[1-\cos\left(2kx\sin\theta+\omega\frac{s}{c}\right)\right]d\omega. \tag{8}$$

We assume that the original spectral density is independent of position so that $S^i(\boldsymbol{r},\omega)=S^i(\omega)$. We thus see that the x-polarized light has an effective spectral density proportional to $S^i(\omega)\{1+\cos[2kx\sin\theta+\omega(s/c)]\}$, whereas the z-polarized light has an effective spectral density proportional to $S^i(\omega)\{1-\cos[2kx\sin\theta+\omega(s/c)]\}$. Thus, we have shown that different polarization components give rise to different spectra which depend on the position in the interference pattern. This fact should be accounted for when studying the spectral characteristics of diverging or converging light in interferometric geometries.

After summing up the contributions from the x and z components, we get the total intensity

$$I(x,\theta) = 2\int_0^\infty S^i(\omega)\left[1+\cos(2\theta)\cos\left(2kx\sin\theta+\omega\frac{s}{c}\right)\right]d\omega, \tag{9}$$

where the total spectral density is given by

$$S(x,\theta,\omega) = S^i(\omega)\left[1+\cos(2\theta)\cos\left(2kx\sin\theta+\omega\frac{s}{c}\right)\right]. \tag{10}$$

When $\theta=45^\circ$ we notice that there is no interference since the two waves are orthogonally polarized, and the original spectral density is retrieved.

To see how the spectrum is modified by the interference, we will now assume that we are located at $x=0$ and that the original spectrum is Gaussian, i.e.,

$$S^i(\omega) = \exp\left[-\frac{(\omega-\omega_0)^2}{\sigma^2}\right]. \tag{11}$$

Figure 2 shows the normalized spectral density [Eq. (10)] for two interfering waves when $\theta=0^\circ$. The dashed line corresponds to the incident Gaussian spectrum $S^i(\omega)$ with center frequency $\omega_0=3\times10^{-15}$ s^{-1} and $\sigma=0.1\omega_0$. The dotted line represents the spectral density found when $s=0.25$ μm, whereas the solid line corresponds to $s=0.45$ μm. From this figure it is seen that as we increase the difference in path-length s the spectrum first experiences a redshift and then a blueshift. If we increase s substantially, we notice that the spectral density exhibits rapid oscillations as we move through the available frequency content. This is seen in Fig. 3, where the solid line is the spectrum found when $s=30$ μm. Now we have multiple peaks with frequency difference (between neighbor peaks) given by $\Delta\omega=2\pi c/s$. The number of peaks generated is approximately given by $N\sim4\sigma/\Delta\omega$, and for $s=30$ μm it is $N\approx19$.

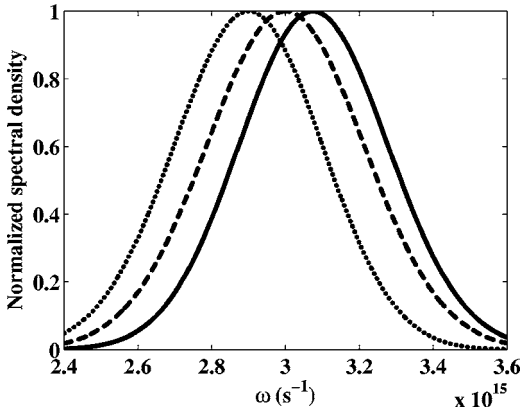

FIG. 2. The figure shows the normalized spectral density for two interfering waves when $\theta=0^\circ$. The dashed line corresponds to the incident Gaussian spectrum $S^i(\omega)$ with center frequency $\omega_0=3\times10^{-15}$ s^{-1} and $\sigma=0.1\omega_0$. The dotted line is the red shifted spectrum found when $s=0.25$ μm, whereas the solid line is the blue shifted spectrum found when $s=0.45$ μm.

The use of interfering waves to investigate the spectrum of lasers and other light sources is a well studied topic, and has been used in spectroscopic systems for decades [14,15]. However, here we point out that an interferometric setup can conveniently modify the spectral characteristics of beams, thus enabling us to tailor the spectral density. In particular we emphasize that the various polarization components may have different spectral densities. To this end, Fig. 4 shows the normalized spectral density for the x (solid line) and z (dotted line) polarization components when $x=0$, $\theta=45^\circ$, and $s=0.25$ μm. The dashed line corresponds to the incident Gaussian spectrum $S^i(\omega)$ with center frequency $\omega_0=3\times10^{-15}$ s^{-1} and $\sigma=0.1\omega_0$. It is seen that while the x component is strongly redshifted, the z component is slightly blueshifted.

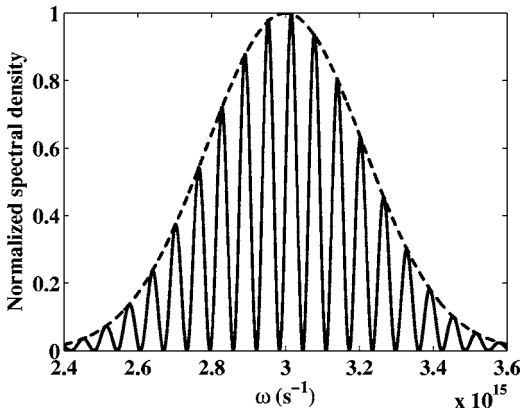

FIG. 3. The figure shows the normalized spectral density for two interfering waves when $\theta=0^\circ$. The dashed line corresponds to the incident Gaussian spectrum $S^i(\omega)$ with center frequency $\omega_0=3\times10^{-15}$ s^{-1} and $\sigma=0.1\omega_0$, whereas the solid line is the spectrum found when $s=30$ μm.

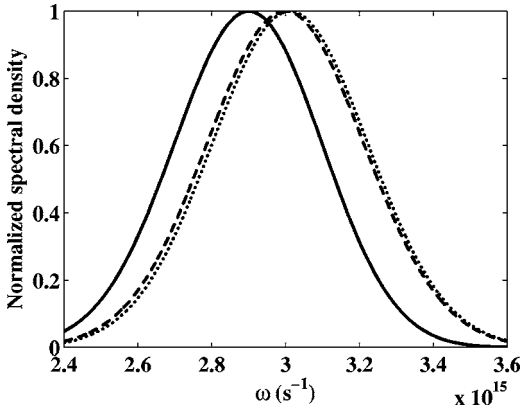

FIG. 4. The figure shows the normalized spectral density for the x (solid line) and z (dotted line) polarization components when $x=0$, $\theta=45^\circ$, and $s=0.25$ μm. The dashed line corresponds to the incident Gaussian spectrum $S^i(\omega)$ with center frequency $\omega_0=3\times10^{-15}$ s^{-1} and $\sigma=0.1\omega_0$. It is seen that while the x component is strongly redshifted, the z component is slightly blueshifted, and their spectra differ considerably.

III. SPECTRAL DENSITY OF FOCUSED WAVES

In the particular case discussed above there is a 180° phase difference between the z polarization components of the two interfering waves which gives rise to a relatively simple change in the spectral density. However, in many situations the polarization distributions are more complex, thus leading to significantly altered intensity distributions and therefore also spectral densities. Here we will take one step further and investigate what happens to the spectral density of the various polarization components when a wave is focused with high angular aperture to a tight focal spot. In order to proceed we will make two approximations. First we will assume that the transmission through the aperture of the high aperture focusing system is independent of the wavelength. Thus, the shape and size of the spatially coherent, incoming beam is only determined by the aperture itself. This is a reasonable approximation if the aperture (of radius a) is overfilled such that the diameter of the input beam is larger than $2a$. We will also assume that the focal length of the system is constant and independent of wavelength. This can be obtained by designing, e.g., a parabolic mirror or a lens system which focuses each wavelength at the same focal point. Using the Debye approximation, the coherent electric field vector of a single spectral component of spectral strength $A(\omega)$ can near the focal plane be expressed as [16,17]

$$\boldsymbol{E}(r,\omega) = -\frac{ikA(\omega)}{2\pi}\int\int_{\Omega}\frac{\boldsymbol{T}(\boldsymbol{s})}{s_z}\exp[ik(s_x x + s_y y + s_z z)]ds_x ds_y, \tag{12}$$

where $k=\omega/c$ is the wave number in vacuum, $\boldsymbol{s}=(s_x,s_y,s_z)$ is the unit vector along a typical ray, Ω is the solid angle formed by all the geometrical rays, $\boldsymbol{T}(\boldsymbol{s})$ is the vector pupil distribution which accounts for the polarization, phase and amplitude distributions at the exit pupil. We emphasize that Eq. (12) is only valid as long as the Fresnel number N is much larger than unity, i.e., $N=a^2/\lambda f \gg 1$, where f is the focal length [17]. Moreover, care must be taken such that the wavelength span of the polychromatic wave does not cause a violation of the requirement $N\gg1$ (the longest wavelength must still give $N\gg1$).

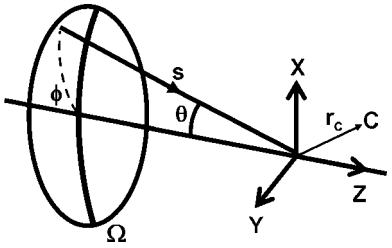

FIG. 5. Schematic drawing of the focusing geometry. Each ray is directed towards the origin of the coordinate system, which coincides with the focal point. The solid angle Ω defines the angular content of the focused rays.

We now consider a circular symmetric focusing system, see Fig. 5. In spherical coordinates, the unit wave vector is defined as

$$\boldsymbol{s} = [\sin\theta\cos\phi, \sin\theta\sin\phi, \cos\theta]. \tag{13}$$

The position vector can be written as

$$\boldsymbol{r}_c = [r_c\sin\theta_c\cos\phi_c, r_c\sin\theta_c\sin\phi_c, z], \tag{14}$$

where we for the rest of the paper set $r=r_c\sin\theta_c$, which represents a projection onto the focal plane. For a system of numerical aperture $NA=\sin\alpha$ Eq. (12) gives the following diffraction integral:

$$\boldsymbol{E}(r,\omega) = -\frac{i\omega A(\omega)}{2\pi c}\int_0^{\alpha}\int_0^{2\pi}\boldsymbol{T}(\theta,\phi)\exp[ikr\sin\theta\cos(\phi-\phi_c) + ikz\cos\theta]\sin\theta\, d\theta\, d\phi, \tag{15}$$

where α is the convergence semiangle and the amplitude vector for each ray is given by

$$\boldsymbol{T}(\theta,\phi) = C(\theta,\phi)\boldsymbol{P}(\theta,\phi). \tag{16}$$

Here $C(\theta,\phi)$ is the transmittance function and $\boldsymbol{P}(\theta,\phi)$ is the polarization distribution, see Refs. [13,18]. It should be noted that $C(\theta,\phi)$ can be applied to any focusing systems. As a special case we also see that if the incoming beam is formed into a bright ring at the exit pupil, it can be described approximately by a delta function $C(\theta)=\delta(\theta-\theta_0)$, where θ_0 is the angular location of the ring at the aperture.

It is important to emphasize that the x, y, and z components are governed by different dependencies on ϕ, which may give rise to different spectral characteristics for each polarization component [13]. In particular we expect highly asymmetric polarization distributions to give rise to different spectra for each polarization component. However, also in the case of symmetric distributions significant spectral anomalies may occur. As an example we first assume a focused scalar wave with $\boldsymbol{P}=(1,0,0)$ and $C(\theta)=\delta(\theta-90^\circ)$, which upon integrating Eq. (15) results in the following spectral density in the focal region:

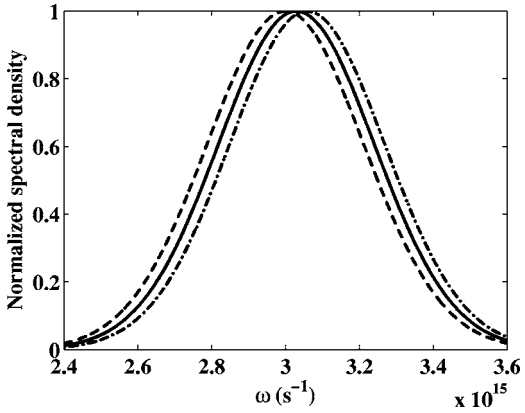

FIG. 6. The figure shows the normalized spectral density for the scalar Bessel beam (solid line) and the azimuthally polarized Bessel beam (dash-dotted line) when $r=0.01$ μm. The dashed line corresponds to the incident Gaussian spectrum $S^i(\omega)$ with center frequency $\omega_0=3\times10^{-15}$ s^{-1} and $\sigma=0.1\omega_0$. It is seen that the azimuthally polarized Bessel beam is more blueshifted than the scalar Bessel beam.

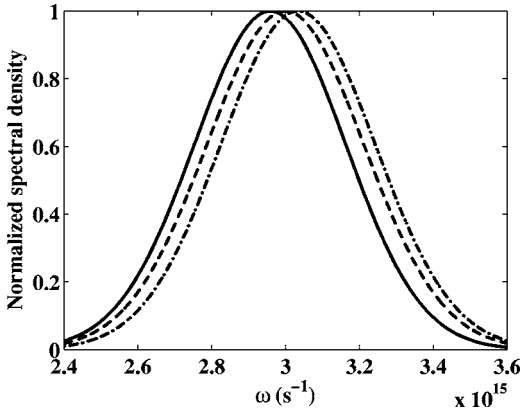

FIG. 7. The figure shows the normalized spectral density for the scalar Bessel beam (solid line) and the azimuthally polarized Bessel beam (dash-dotted line) when $r=0.17$ μm. The dashed line corresponds to the incident Gaussian spectrum $S^i(\omega)$ with center frequency $\omega_0=3\times10^{-15}$ s^{-1} and $\sigma=0.1\omega_0$. It is seen that the azimuthally polarized Bessel beam is blueshifted while the scalar Bessel beam is redshifted.

$$S^{\mathrm{sc}}(\omega)=\omega^2 S^i(\omega)J_0^2\left(\frac{\omega}{c}r\right), \tag{17}$$

where $J_0(\omega r/c)$ is a Bessel function of the first kind and order 0 and $S^i(\omega)$ is the spectral density of the beam entering the focusing system $[S^i(\omega)\propto|A(\omega)|^2]$. On the other hand, if we consider an azimuthal polarization distribution with $\boldsymbol{P}=(\sin\phi,-\cos\phi,0)$ and $C(\theta)=\delta(\theta-90^\circ)$ we obtain the following spectral density in the focal region:

$$S^{\mathrm{az}}(\omega)=\omega^2 S^i(\omega)J_1^2\left(\frac{\omega}{c}r\right), \tag{18}$$

where $J_1(\omega r/c)$ is a Bessel function of the first kind and order 1. Both Eqs. (17) and (18) belong to the class of "diffraction free" beams discussed in Refs. [19,20] (see also Refs. [13,21]), and there is almost no broadening of the beam in the vicinity of the focal plane. It is also easy to see that they produce very different spectral densities in the focal region. When $r\ll c/\omega$, we notice that $S^{\mathrm{sc}}\propto\omega^2 S^i(\omega)$ while $S^{\mathrm{az}}\propto\omega^3 S^i(\omega)$, and an azimuthal polarization distribution will therefore be more blue shifted at very small distances. This is seen in Fig. 6, where the normalized spectral densities are displayed for $r=0.01$ μm. The dashed line corresponds to the incident Gaussian spectrum [Eq. (11)], with center frequency $\omega_0=3\times10^{-15}$ s^{-1} and $\sigma=0.1\omega_0$. Upon moving further away from the optical axis, it is seen that the spectral density of the scalar bessel beam starts to decrease more rapidly with increasing frequency thus resulting in a net redshift. On the other hand, it can be shown that Eq. (18) obtains its maximum value when $r=0.15$ μm for the largest frequency in the incident Gaussian spectral density, and the azimuthal spectral distribution will only be redshifted when $r>0.25$ μm. This situation is depicted in Fig. 7, where the normalized spectral densities are displayed for $r=0.17$ μm. Here the scalar Bessel beam is redshifted while the azimuthally polarized Bessel beam is blueshifted.

As discussed in Refs. [2,4] spectral singularities occur in regions of zero intensity. This phenomenon can be noted from Fig. 8, which shows the normalized spectral density for the scalar Bessel beam (solid line) and the azimuthally polarized Bessel beam (dash-dotted line) when $r=0.22$ μm. It is seen that the spectral density of the azimuthally polarized Bessel beam is nearly identical to that of the incident beam (Gaussian distribution), while the scalar Bessel beam is strongly redshifted. Also shown is the normalized spectral density for the scalar Bessel beam when $r=0.26$ μm (dotted line), and in this case the spectrum is strongly blueshifted. The quick spatial change from redshift to blueshift is a sign of a spectral singularity [2,4,6].

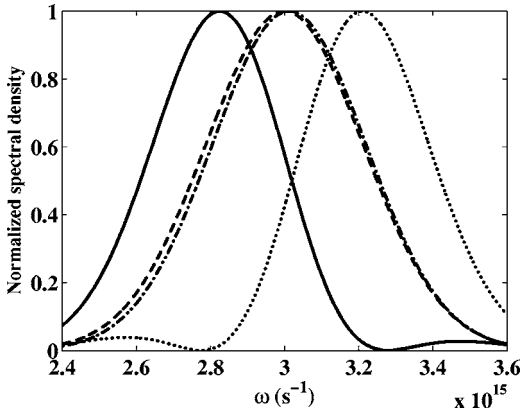

FIG. 8. The figure shows the normalized spectral density for the scalar Bessel beam (solid line) and the azimuthally polarized Bessel beam (dash-dotted line) when $r=0.22$ μm. The dashed line corresponds to the incident Gaussian spectrum $S^i(\omega)$ with center frequency $\omega_0=3\times10^{-15}$ s^{-1} and $\sigma=0.1\omega_0$. It is seen that the spectral density of the azimuthally polarized Bessel beam is nearly identical to the incident Gaussian distributions, while the scalar Bessel beam is strongly redshifted. Also shown is the normalized spectral density for the scalar Bessel beam when $r=0.26$ μm (dotted line), and it is clear that now the spectrum is strongly blueshifted.

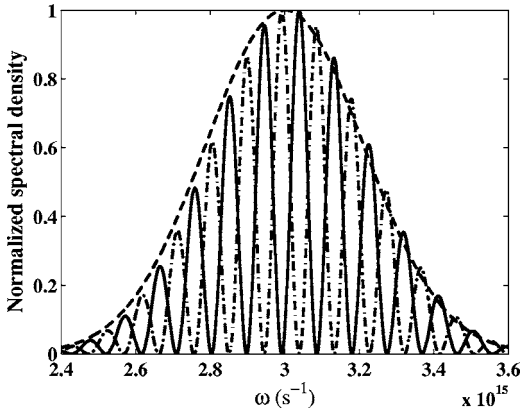

FIG. 9. The figure shows the normalized spectral density for the scalar Bessel beam (solid line) and the azimuthally polarized Bessel beam (dash-dotted line) when $r=10\ \mu$m. The dashed line corresponds to the incident Gaussian spectrum $S^{i}(\omega)$ with center frequency $\omega_0=3\times10^{-15}\ \mathrm{s}^{-1}$ and $\sigma=0.1\omega_0$.

If we move far away from the optical axis, it is interesting to note that the Bessel functions oscillate more rapidly as we scan through the frequency range of the polychromatic waves, and several regions of zero intensity may be available. This phenomenon is equivalent to that observed in the previous section, where an increase in the path difference $s=c\tau$ resulted in oscillations of the spectral density. Figure 9 shows the normalized spectral density for the scalar Bessel beam (solid line) and the azimuthally polarized Bessel beam (dash-dotted line) when $r=10\ \mu$m. As in Fig. 3, multiple peaks are observed in the spectrum, although slightly shifted away from the center of the Gaussian envelope due to the decaying nature of the Bessel functions. We also note that peaks of the scalar and azimuthally polarized Bessel beams are almost out of "phase" such that when $S^{\mathrm{sc}}(\omega)$ is at its maximum then $S^{\mathrm{az}}(\omega)$ is at its minimum. This effect could be used in designing focused light with localized spectral characteristics, where the incident polarization distribution determines the position of the peaks as seen in Fig. 9.

IV. CONCLUSION

We have studied the influence of phase shifts and polarization distributions on the spectral density of polychromatic electromagnetic waves. We found that the different polarization components in general have different spectral characteristics, thus leading to a spectral density that differs from the scalar case. We suggest that these effects can be used to design spatially located spectra with tailored spectral densities.

[1] J. Pu, H. Zhang, and S. Nemoto, Opt. Commun. **162**, 57 (1999).
[2] G. Gbur, T. D. Visser, and E. Wolf, Phys. Rev. Lett. **88**, 013901 (2002).
[3] G. Popescu and A. Dogariu, Phys. Rev. Lett. **88**, 183902 (2002).
[4] G. Gbur, T. D. Visser, and E. Wolf, J. Opt. Soc. Am. A **19**, 1694 (2002).
[5] J. T. Foley and E. Wolf, J. Opt. Soc. Am. A **19**, 2510 (2002).
[6] J. Pu, C. Cai, and S. Nemoto, Opt. Express **12**, 5131 (2004).
[7] E. Heyman, B. Z. Steinberg, and L. B. Felsen, J. Opt. Soc. Am. A **4**, 2081 (1987).
[8] M. A. Porras, R. Borghi, and M. Santarsiero, Phys. Rev. E **62**, 5729 (2000).
[9] G. P. Agrawal, Opt. Commun. **167**, 15 (1999).
[10] M. A. Porras, Opt. Lett. **26**, 1364 (2001).
[11] M. A. Porras, Phys. Rev. E **65**, 026606 (2002).
[12] Z. J. Liu and B. D. Lu, Opt. Commun. **206**, 13 (2002).
[13] L. E. Helseth, Phys. Rev. E **72**, 047602 (2005).
[14] H. Welling and B. Wellegehausen, Appl. Opt. **11**, 1986 (1972).
[15] C. N. Banwell and E. M. Cash, *Fundamentals of Molecular Spectroscopy* (McGraw-Hill, New Delhi, 1994).
[16] P. Debye, Ann. Phys. **30**, 755 (1909).
[17] J. J. Stamnes, *Waves in Focal Regions* (Adam Hilger, Bristol, 1986).
[18] L. E. Helseth, Opt. Commun. **212**, 343 (2002).
[19] J. Durnin, J. J. Micelli, and J. H. Eberly, Phys. Rev. Lett. **58**, 1499 (1987).
[20] S. Orlov and A. Stabinis, Opt. Commun. **240**, 1 (2004).
[21] In Ref. [13], page 2 right after Eq. 14, it should have been emphasized that the discussion of "diffraction free" beams is referring to the spectral (monochromatic) components only. In the case of a polychromatic pulsed beam it is seen from Eqs.(12–14) in Ref. [13] that the electric field depends on both r and z in a nontrivial manner.